Monte Carlo simulations of a surface reaction model showing spatio-temporal pattern formations and oscillations

Monte Carlo simulations of a surface reaction model showing spatio-temporal pattern formations and oscillations

R. J. Gelten, A. P. J. Jansen, and R. A. van Santen
Eindhoven University of Technology, Schuit Institute of Catalysis, P.O. Box 513, 5600 MB Eindhoven, The Netherlands

J. J. Lukkien and J. P. L. Segers
Eindhoven University of Technology, Department of Mathematics and Computing Science, P.O. Box 513, 5600 MB Eindhoven, The Netherlands

P. A. J. Hilbers
Eindhoven University of Technology, Schuit Institute of Catalysis, and Department of Mathematics and Computing Science, P. O. Box 513, 5600 MB Eindhoven, The Netherlands

(Received 26 December 1996; accepted 2 December 1997)

Results of dynamic Monte Carlo simulations of a model for CO oxidation on a reconstructing Pt(100) surface are presented. A comparison is made between simulations that explicitly include surface diffusion of adsorbed CO and simulations without diffusion. Oscillatory behavior as well as spatio-temporal pattern formation are studied as a function of system size. In the absence of diffusion the amplitude of kinetic oscillations decreases with grid size and oscillations are not stable. Spatio-temporal patterns appear, as expected for an excitable medium. Such patterns become stabilized by structural substrate defects. The length scale of the patterns is in the order of 10–100 nm, the temporal period of the oscillations is around 200 seconds. Inclusion of diffusion stabilizes and synchronizes oscillations. Spatio-temporal features now appear with larger spatial dimensions. © *1998 American Institute of Physics.* [S0021-9606(98)00510-8]

I. INTRODUCTION

Reaction rates on catalytically active metals are controlled by the complex interplay of rate constants of the elementary reaction steps and composition and structure of the surface overlayer. The latter may change with reaction conditions, such as the composition of reactant gas phase pressure and temperature. Mixing of the adsorbed reaction intermediates often has to be considered non-ideal. Ordered overlayers can appear due to lateral interactions between chemisorbed atoms and molecules and surface reconstructions. The consequences of these effects on overall kinetic behavior are often very complex. Methods to analyze the effects of surface coverage and surface reconstruction on catalytic activity are therefore an important topic of research.

Recently, methods have become available that enable computation of the elementary rate constants of chemical reactions between adsorbed atoms and molecules. They are based on the use of transition state reaction rate theory and employ potential energy surfaces that can be deduced from quantum chemical calculations.[1–5] Complemented with statistical mechanical methods that solve the many particle problem for the surface, this in principle should make the *ab initio* prediction of the rate of heterogeneous catalytic reactions possible, including the phenomena that are the result of non-ideal mixing behavior in the surface adlayer.

The use of time dependent, or dynamic, Monte Carlo techniques[6,7] in surface catalysis has been developed in recent years.[8–12] The advantage of these methods is that experimentally observed kinetic behavior can be used to compare with simulated results. Our goal in this study is to use these time dependent Monte Carlo model simulations to analyze the microscopic basis of synchronized kinetic oscillations and spatio-temporal pattern formations such as found in the oxidation of CO on platinum single crystal surfaces. This reaction has been chosen because a wealth of existing experimental and theoretical results that exists for this system.[13–15]

In order to do this, we have developed a model system that makes a detailed time dependent Monte Carlo simulation of the CO oxidation on a reconstructing surface possible. The choice of the reaction types were determined by experimental and theoretical findings on the CO oxidation on platinum single crystals. The choices for the values of the reaction rates were based on the CO oxidation on Pt(100). In these experiments, the oxidation rate is found to oscillate in a particular temperature and pressure regime.[13–15] This oscillatory behavior has been ascribed to surface reconstruction[16,17] that is a function of adlayer composition. Our simulations reproduce the experimental oscillatory regime as well as the period of the oscillations, and sustain the conclusion that surface reconstructions drive the oscillations on the Pt(100) surface. Some of the spatio-temporal pattern formations observed in experiments on platinum surfaces were reproduced qualitatively. The length scale of these phenomena in our simulations, however, is much smaller than experimentally observed.[18,19] The length scales appear to depend strongly on the inclusion of diffusion in our model.

Many other models have been used for MC simulations in the literature and CO oxidation on platinum single crystal surfaces is often used for reference in those studies. The most simple model is the Ziff–Gulari–Barshad (ZGB)

model,[20] which includes only adsorption of CO, dissociative adsorption of O_2 and reaction between CO_{ads} and O_{ads}. The aim of this model was to simulate the kinetic phase transitions, observable through the steady state coverages of CO_{ads} and O_{ads}.

Not many Monte Carlo models have been used to simulate kinetic oscillations in catalysis[21–32] and several of these studies have the problem that they describe oscillations on very small systems of less than two thousand sites.[21–23,25] In this study we show that finite size effects will often be observed on grids with millions of sites and that simulations on small grids only give information on local fluctuations. Models which aimed to simulate the oscillations in CO oxidation include extra reaction steps which provide the necessary feedback mechanism.

One way to induce these oscillations is by introducing an inert species which blocks surface sites.[29,32,33] Accumulation and removal of this species is slow compared to the other relevant processes. The carbon model,[34,35] the oxide model[34–36] and the subsurface oxygen model[37,38] are well known examples of such models.

Some other models include reconstruction of the substrate surface. MC simulations with these models have shown irregular oscillations on rather small grids.[21,24,39,40] On the basis of the results presented in this paper, it is likely that these oscillations will vanish on large grids.

Most of the results to be presented here are based on models that do not include a communication mechanism which can provide the necessary feedback for synchronization of local oscillators in our model. Especially diffusion can play a role in this process. Therefore, we will briefly discuss some initial results of simulations which do include diffusion in Sec. IV D and compare them with results obtained without explicit diffusion.

A main result of this paper is the simulation of cellular patterns that occur during oscillations. Such patterns have not earlier been reported from Monte Carlo simulations. Dynamic creation of target patterns was also simulated. Finite size effects of the grids are carefully analyzed and shown to extend up to very large grids (millions of sites). The simulations with diffusion included in the model confirm that diffusion provides an important synchronization mechanism.

II. SIMULATION TECHNIQUE

Several methods can be used to study kinetics of catalytic reactions theoretically. Mean-field modeling with ordinary differential equations (ODEs), for example, is a very powerful method. Many general features of the CO oxidation on single crystal surfaces have been investigated thoroughly with this method.[17,37,38,41–44] Extension of the ODE description with diffusional terms (reaction-diffusion equations) allows modeling of spatio-temporal pattern formations. However, these methods are fundamentally limited in the sense that it always considers *average* environments of molecules or reactive sites.

This approximation is overcome in Monte Carlo (MC) simulations, where local environments can be specified exactly. Moreover, if we want to simulate the behavior of such systems stochastically on time scales of chemical reactions, MC simulation is the only feasible method. In this report, we use the MC method to study influence of microscopic reactions and fluctuations on macroscopic or mesoscopic phenomena.

A current practical limitation of this method is encountered when a reaction occurs a lot more often than other reactions. In our case, this causes a problem because fast diffusion processes cannot be simulated with the size of grids necessary to simulate local synchronization. The reason is that with increasing diffusion rates, increasingly much computation time is spent on diffusion, whereas the reaction of interest to us is CO_2 production. The practical limit for the diffusion rate strongly depends on the complexity of the model and the grid size. Usually, the diffusion rate for dynamic MC simulations can be up to 100–1000 times faster than the other reactions in the model.

We distinguish MC simulations from regular cellular automata; in the latter all reactive sites perform transitions synchronously. This internal synchronization makes these automata very suitable for simulation of pattern formation on surfaces, such as rotating spirals and target patterns.[45,46] However, these patterns are partially a result of the simulation method itself. Furthermore, unless the simulation scheme of the cellular automaton is corrected, these methods have no physical meaning as they discard the global notion of time in contrast to Monte Carlo simulations where reactions occur at the correct time. A more sophisticated use of the MC technique is provided in dynamic Monte Carlo (DMC) simulations in which the time dependence is correct and the behavior of a catalytic system is simulated in real time. In these simulations, experimental data can be used directly for comparison or as system parameters.

The simulations used here are of the DMC type. They are based on the following master equation:

$$\frac{dP_\alpha}{dt} = \sum_\beta \left(W_{\beta\to\alpha}P_\beta - W_{\alpha\to\beta}P_\alpha\right), \tag{1}$$

where P_α (P_β) is the probability of finding the system in configuration α (β). A configuration is an assignment of particles to a grid which models the catalytically active surface and the adsorbed particles. An example of such a configuration is a square grid of 10×10 sites, with an adsorbed CO molecule on every site. The W's are transition probabilities per unit time for various reactions. These may include reactions such as adsorption, desorption, etcetera. In this study the W's are time independent. We have used three equivalent methods to solve this master equation: the first reaction method (FRM), the variable step size method (VSSM) and the random selection method (RSM).[6,7,12] We will briefly explain these methods.

Suppose that at time t the system is in configuration α. We may compute the set of all possible reactions. Time intervals $\Delta t_{\alpha\to\beta}$ are generated for all of these reactions, β being the configuration of the system after performing the reaction in configuration α. For example, α is an empty grid of 10×10 sites, β is the same grid with a CO molecule adsorbed on a specific site. From the master equation, we can derive that these time intervals $\Delta t_{\alpha\to\beta}$ have exponential dis-

tributions with parameters $W_{\alpha\to\beta}$. Hence they can be generated according to the following formula:

$$\Delta t_{\alpha\to\beta} = -\frac{1}{W_{\alpha\to\beta}} \ln r_{\alpha\to\beta}. \tag{2}$$

Here $r_{\alpha\to\beta}$ is a random number selected uniformly in the interval (0,1) for every transition $\alpha\to\beta$. The reaction with the smallest waiting time is performed, i.e., the configuration is adapted, and time is incremented by $\Delta t_{\alpha\to\beta}$. The set of possible reactions is now adapted to account for any reactions that have become possible or impossible as a result of the transition. This whole procedure of selecting a reaction, adapting the configuration and adapting the set of possible reactions is repeated. This method is called FRM.

In VSSM only one waiting time is generated, according to

$$\Delta t = -\frac{1}{\Sigma_\beta W_{\alpha\to\beta}} \ln r, \tag{3}$$

again with r a random number selected uniformly from (0,1). Time is incremented by an amount Δt. Next one reaction is selected from the set of all possible reactions, with a probability proportional to its rate $W_{\alpha\to\beta}$ (again β is the resulting configuration of the reaction). The selected reaction is performed and the set of possible reactions is adapted to take the changes on the grid into account. This procedure is repeated.

The RSM is used quite often in the literature, although mostly without use of correct time dependence. In this method, a site is selected with probability $1/N$, where N is the total number of sites. After that, a reaction type i (e.g. CO adsorption or desorption) is selected with probability $r_i/\Sigma_i r_i$, where r_i is the rate of reaction type i. When the selected reaction type is possible on the site, it is executed. After each selection of a site, time is incremented by Δt, which is selected from a fixed distribution $1-\exp(-Nt\Sigma_i r_i)$:

$$\Delta t = -\frac{1}{N\Sigma_i r_i} \ln r. \tag{4}$$

An easier way to include real time in RSM is to increment time by a fixed amount given by the mean of equation (4). The difference between this method and using equation (4) washes out after just a few steps. However, one should be careful with this simplified method as it can introduce artifacts when one would want to calculate time-correlation functions. Also when one would want to simulate with time-dependent rate constants, the more general RSM (or FRM) should be used.

FRM and VSSM can be implemented very efficiently, because information generated at some time step can be reused at subsequent steps. A detailed analysis of the three methods and their equivalence is published elsewhere.[12] The advantage of VSSM and RSM over FRM is that the cost per generated transition (reaction) is independent of the size of the grid used in the simulation, whereas in FRM it scales as the logarithm of the number of grid points. This makes the method more efficient in memory use and execution time than FRM for large grids. The advantage of FRM over VSSM is that it is a suitable method to simulate reactions with time-dependent transition probabilities, as in temperature programmed desorption experiments. However, we have not made use of this feature in the work presented here. The advantage of RSM is that is easy to implement and for some models (or reaction types) it is a very fast method.

Two general-purpose programs have been developed in our groups. One, PIZZAZZ,[47] implements FRM, and the other one, CARLOS,[48] implements FRM, VSSM and RSM. In CARLOS, RSM and VSSM can be used for different reaction types within one model, which can speed up the simulations considerably. Especially in simulations where we have included diffusion, a speed up by a factor of 2 could be obtained.

Simulating diffusion is one of the major problems in MC simulations. When diffusion is taken into account, the most often used approaches are to allow a fixed number of diffusion steps after each reaction,[40] or relax the configuration to equilibrium after each reaction.[49,50] Another approach is formed by the class of hybrid models[51] in which the effects of diffusion are treated with a non-Monte Carlo method, e.g. modeling with ODEs. These approaches are mostly less expensive than treating diffusion correctly, i.e. by considering diffusion as a normal reaction with a certain rate (probability). However, these methods are approximations and can have serious drawbacks like assuming uniform distributions of adsorbates, even if sites are topologically disconnected.[51] We have chosen for the rigorous approach, which has the major drawback that only slow diffusion rates can be used. The advantage of this method is that it is precise.

III. MODEL

A. Description

We have simulated oscillating chemical reactions occurring on a catalytically active reconstructing single-crystal surface. As a reference for discussion, we take the CO oxidation on the Pt(100) crystal plane. There are few MC studies dedicated to oscillations in CO oxidation rates on single crystal surfaces[24,26–32] and our present model can be viewed as an extension of some of those models.

In the absence of adsorbates, the top layer of the Pt(100) surface has a reconstructed hexagonal structure, which can be considered a corrugated (111) surface. Adsorbates such as CO are known to be able to lift this reconstruction, upon adsorption above a certain threshold coverage.[52,53] The surface then transforms into the truncated bulk structure (1×1 phase), which is a square lattice. The difference between the sticking coefficients of oxygen on both phases causes the oscillations; because oxygen adsorption is a thousand times faster on the 1×1 phase, CO_2 production occurs only on that phase. From experiments, it is known that the surface transformation from hexagonal into 1×1 phase and vice versa switches the system from an unreactive phase into a reactive one, and back. The cause of the transformation lies in the somewhat higher heat of adsorption of CO on the square lattice.[53,54] Several reports suggest a nucleation and growth mechanism for this transformation.[54–58] King and coworkers suggested a nucleus size around four to five.[59,60]

Reactions are simulated on a regular grid with periodic boundary conditions. We will model the reconstruction and

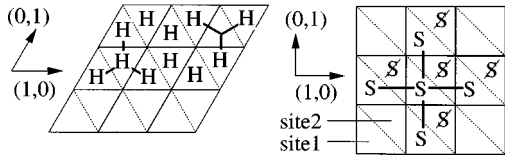

FIG. 1. Illustration of neighbor relations between the sites. Unit cell boundaries are indicated with solid lines, site boundaries with dotted lines. Thick lines show the neighbor relations on the hexagonal and 1×1 phases. Blocked sites are indicated with crossed out labels. For representation purposes, we have drawn the unit cells for the hexagonal phase in an oblique fashion, so that the neighbor relations become more obvious. For the simulation, only the numerical coordinates (x, y) are important. Unit vectors are only used for graphical representations.

all other processes on a single grid. The grid consists of unit cells with two sites. Labels ''H'' and ''S'' on the sites indicate the surface phase (hexagonal and 1×1, respectively). Different neighbor relations hold for the two phases; a site on the 1×1 phase has four neighbors, a site on the hexagonal phase has three neighbors, as shown in Fig. 1. We indicate the three coordinates of a site with (x, y, s), where x and y stand for the coordinates of the unit cell in the directions indicated in the figure, and s stands for the number of the site ($s=1$ or $s=2$). On the hexagonal grid, all H-labeled sites can be occupied by adsorbates. Thus, we see that on the hexagonal phase the neighbors of site $(0,0,1)$ have relative coordinates $(0,0,2)$, $(-1,0,2)$ and $(0,-1,2)$. The neighbors of site $(0,0,2)$ have relative coordinates $(0,0,1)$, $(1,0,1)$ and $(0,1,1)$. On the square lattice the neighbor relations are different. We block one of the sites in this phase. By convention, we block sites 2, which means that this site is not available for any adsorbate and merely acts as a label, indicating that site 1 is in the 1×1 phase. Neighbors of sites 1 have relative coordinates $(1,0,1)$, $(-1,0,1)$, $(0,1,1)$ and $(0,-1,1)$. Hence, on the square lattice, sites have four neighbors and on the hexagonal lattice, each site has three neighbors. Effectively, the two sites of the unit cell correspond to one site on the square lattice.

If we imagine surface metal atoms on the vertices in Fig. 1, we see that, with the neighbor relations as we defined them, the sites correspond to hollow sites on the hexagonal (H labels) and the 1×1 phase (S labels). Adsorption of CO on top sites instead of hollow sites does not have a significant influence on the results described in this report. If we would wish to consider linear (atop) bonding sites instead of hollow sites, we would need new neighbor relations for the hexagonal phase, because in this case every site has six neighbors instead of three. This can be done by adsorbing species on sites 1 only (never on sites 2), and using sites 2 as a phase label on both phases. If we then imagine site 1 to be located on top of the substrate atoms (the vertices in Fig. 1), we see that we find a sixfold neighbor relation. This sixfold symmetry is then accounted for in the reaction specifications.

Note from Fig. 1 that the (square) 1×1 phase and the hexagonal phase have different unit vectors. For the simulation program, this is not a problem, because it only uses relative coordinates of the sites that are involved in a reaction. However, in the physical system this implies a misfit between the phases. Furthermore, the hexagonal phase has a 20% higher site density than the 1×1 phase. In the physical system, the excess platinum atoms are pushed out from the surface during the hexagonal $\rightarrow$ 1×1 reconstruction. These platinum atoms gather in unreactive islands. The islands disappear in the reverse reconstruction.[50] In our simulations, these effects are ignored. The phase boundaries form no barrier for any reaction in our model, despite the misfit. It is assumed that excess platinum atoms are always available to prevent macroscopic deformations of the lattice due to reconstructions.

We will now briefly describe our model in terms of reactions between CO and O_2, where CO can adsorb on and desorb from both the square and the hexagonal phase. O_2 can dissociatively adsorb on neighboring unit cells of the 1×1 phase only (we have set the very low sticking coefficient of oxygen on the hexagonal phase to zero). Oxygen atoms are bound so strongly that associative desorption can be ignored. Reactions of the type $CO_{ads} + O_{ads} \rightarrow CO_{2,gas}$ can occur between neighboring unit cells. Finally, reactions are specified which control the surface transformations from hexagonal into square and vice versa. For the hex $\rightarrow 1\times1$ reconstruction, a cluster of five CO adsorbates on neighboring positions is required.[59,60] However, when CO is adsorbed on a hexagonal site next to a 1×1 island, this site can be transformed into the 1×1 phase (island growth by trapping). For the reverse reconstruction, one empty unit cell is enough as energy is released in this process.

All reactions are specified as a change of the labels on one or more sites. For example, if CO adsorbs on a hexagonal site, the H label is changed into a CO label. If it adsorbs on a square site, the S label on site 1 is changed into a ''CO,'' while the S label on site 2 is not changed. Desorption of CO changes the label back into an H or S label, depending on the phase of the grid at that spot. For desorption of CO from site 1, site 2 is used as a reference; if it is labelled S, desorption leaves an S label, otherwise it leaves an H label. Desorption of CO from site 2 (in the hollow site model) always leaves an H label, as a CO adsorbed on site 2 can only be on the hexagonal phase. There is only a limited number of combinations of labels within a unit cell: (site 1, site 2)=(S, S) indicates an empty 1×1 site. (CO, S) represents a CO molecule adsorbed on a 1×1 site and (O, S) is the same for oxygen. Other possibilities are (H, H), denoting two empty hexagonal sites, and (CO, H) and (H, CO), both indicating a CO adsorbed on a (hexagonal) site with an empty hexagonal neighbor. The last combination is only possible in the hollow site model. No other combinations are allowed and their occurrence is prevented in the specification of the reactions. A few examples of reactions are sketched in Fig. 2.

We require that no more than one CO molecule can adsorb in each unit cell. For the hollow site model, this means that for a CO molecule to adsorb on a hexagonal site, its hexagonal nearest neighbor sites must be empty. This also prevents the molecule from adsorbing in quantities larger than one monolayer (one monolayer being defined as one adsorbate per surface metal atom). Neighboring square sites may be occupied by any adsorbate. For adsorption on the square phase, the only requirement is that both sites 1 and 2

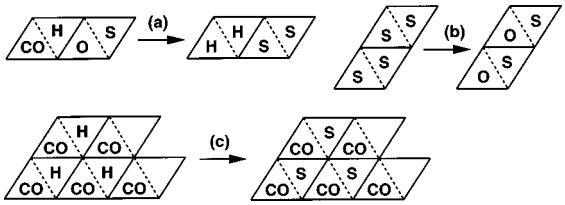

FIG. 2. A few examples of reactions as they are specified in our model. (a) CO oxidation reaction in which a CO molecule on the hexagonal phase reacts with an oxygen atom on the 1×1 phase, (b) dissociative oxygen adsorption on two neighboring 1×1 sites, (c) nucleation. For nucleation, only three H labels are specified to prevent anisotropy. The sites that have no label in the figure may have either an S or an H label.

of a unit cell have label S. CO then adsorbs on site 1.

The rates of the reverse reactions that are not specified in the model are so slow that they can safely be neglected. Adsorbate diffusion is not included in the model presented above. The influence of diffusion on our results will be studied separately.[61] Only first results from simulations which include diffusion will be presented in Sec. IV D.

B. Limitations of the model

One of the limitations of our model is that it does not account correctly for the difference in surface site densities between the hexagonal and the 1×1 phase, which is around 20%. In the hollow-site model described in detail above, the site density on the square phase is 50% smaller than on the hexagonal phase. In the top-site model, the site densities are equal.

The maximum adsorbate coverage in our model is one adsorbate per unit cell, which is too high. Formally, a redefinition of the unit cell size and geometry in our model could correct this. A more explicit adaptation of our model can also be used to correct this limitation, but this would only complicate the present discussion. Another way to prevent these high coverages could be by including explicit lateral interactions between adsorbates. In our study, such interactions are ignored. The only way lateral interactions play a role in our model is through the substrate reconstructions.

In the present model, we have ignored CO adsorption on oxygen precovered areas. From experiments, it is known that CO does adsorb on oxygen covered areas of the Pt(100) crystal, although slower than on a clean surface.[62]

In order to reduce the number of parameters in our model, we have ignored anisotropic effects, although anisotropic nucleation and growth has been observed experimentally on Pt(100).[56,58]

A few choices restrict our model to the Pt(100) surface. First, the symmetry difference between the two phases is as on the reconstructing Pt(100) surface. However, variation of the symmetry of the phases has little influence on the results. Formally, the symmetry changes as in the reconstructing Pt(110) surface are not qualitatively different. The Pt(110) surface has a more complicated geometry to implement in our model, but this may not alter the qualitative results of our simulations. However, the choices we made for the nucleation reactions, such as nucleus size and nucleus configurations, are based on the Pt(100) surface, and a different choice, e.g. for the Pt(110) surface will influence the results at least quantitatively, but perhaps also qualitatively. Finally, the choice for the rate parameters of the elementary reactions limits our results to a certain crystal plane. The main difference between the Pt(100) plane and other reconstructing platinum crystal planes is that the oxygen sticking coefficient varies more on the Pt(100) plane upon reconstruction. Several adaptations to our model would be needed to simulate the oscillatory behavior on the Pt(110) surface or any other single crystal surface. Most of the changes would be in the choice for the rate parameters of the elementary reactions.

Diffusion is not incorporated in most of our simulations. Initial results of some simulations which do include diffusion will be briefly discussed in Sec. IV D. In these simulations, the model included diffusion as a reaction in which CO and an empty site swap positions: $CO+*\rightarrow *+CO$. The problem with this approach is that only much slower than realistic diffusion rates can be used. Faster diffusion rates would require some sort of hybrid model as in Ref. 51. However, a rigorous inclusion of slow diffusion produces interesting results which can be of relevance to high diffusion rates. Although we shall discuss the effects of diffusion briefly in

TABLE I. Comparison between experimental parameters and simulation parameters. p stands for pressure, ν for prefactors, E_{act} for activation energy and S_0 for the initial sticking coefficient. In our model, CO adsorption occurs on both the hexagonal and the 1×1 phase, with equal rates. Parameters for O_2 ads. are for dissociative oxygen adsorption on the 1×1 surface only. Adsorption of oxygen on the hexagonal phase is neglected, since it is a thousand times slower (Refs. 72,73) than on the 1 × 1 phase. Oxygen desorption does not occur, because of the strong bonding of the fragments to the surface. The surface reconstructions are described in the text.

Reaction	p^{sim} (Pa)	p^{exp} (Pa)	S_0^{sim}	S_0^{exp}	Ref.
CO ads.	$1.3\cdot10^{-3}$	$(1–4)\cdot10^{-3}$	0.8	≈0.8	55,72,74
O_2 ads.	$5\text{-}15\cdot10^{-2}$	$2.7\cdot10^{-2}$	0.1	≈0.1	72,73
	ν^{sim} (s^{-1})	ν^{exp} (s^{-1})	E_{act}^{sim} (kJ/mol)	E_{act}^{exp} (kJ/mol)	Ref.
CO des.	$1\cdot10^{15}$	$(1–3)\cdot10^{15}$	175	117–159	52,53,72,74–76
CO_2 prod.	$2\cdot10^{10}$	10^{10}	84	50–100	77
1×1 → hex	$1\cdot10^{9}$	-	105	105	76,78
Nucleation	0.03	-	0	≈ 0	52,53,74,76
Trapping	0.03	-	0	≈ 0	74,76

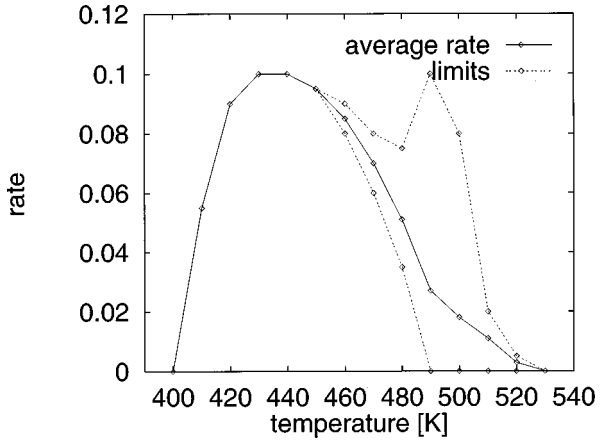

FIG. 3. CO_2 production rate (molecules CO_2 per Pt atom per second) versus temperature. The solid line indicates the average rate. In the oscillatory region, two extra, dashed, curves are drawn: one for the maximum rate (top of oscillations peaks) and one for the minimum rate. The amplitude of the oscillations in this region is then given by the difference between the two dashed curves. The grid size was 256×256. Larger grids did not change the plot significantly.

Sec. IV D, this subject is the main topic for another study.[61]

Finally, we stress that this study contains a limited model description of the CO oxidation on platinum single crystal surfaces. Despite the severe limitations of our model, the simulations will be valuable for the development of more realistic models and provide important new insights into the micro-physics behind observed phenomena.

IV. RESULTS

A. Parameter dependence

The experimental values of the elementary rate constant parameters of the CO oxidation reaction are shown in Table I, together with the parameters used in the simulations. The experimental values inserted in the table, are from single crystal experiments performed under (ultra) high vacuum conditions. No parameters were available for the nucleation and trapping rates, other than the information that the activation barriers should be low. The prefactors for these reactions should be viewed as effective reaction rates, which are assumed to be temperature independent in the temperature range considered. These rates for reconstruction and the CO desorption rate were used as system parameters and they were chosen such that oscillations in the CO_2 production rate were obtained. Values for the temperature and pressure regime as well as for the oscillation period then automatically followed. They were not subject to any fitting procedure.

The kinetic behavior of the system strongly depends on temperature, as shown in Fig. 3. Below 400 K, surface poisoning occurs, and hence the CO_2 production rate is zero. Poisoning occurs by CO or oxygen, depending on the partial pressures and the sticking coefficients used at these temperatures. Between 400 K and 440 K, the CO_2 production rate increases, because of a better balance between CO and oxygen coverage. At temperatures higher than 440 K the average reaction rate decreases, going to zero at 530 K. Adsorption limitations are the cause of the decrease in rate. At temperatures between 470 and 510 K, oscillations are observed. The gradual splitting of the curve in Fig. 3 indicates that we have an Andronov–Hopf bifurcation. We will discuss the different regions in more detail below.

The most interesting temperature range lies between 470 and 510 K, since in this region oscillations in the rate of CO_2 production occur. An example of such oscillations is shown in Fig. 4. From this figure, we see that the period of oscillation in our simulations lies around 200 seconds. The period hardly varies with temperature, although it can be varied by changing some of the parameter values.

Oscillations were observed for a wide range of gas pressures for CO and O_2 adsorption. A minimum O_2 pressure of $1.6 \cdot 10^{-2}$ Pa was required, and at that pressure, the minimum CO pressure was $2.0 \cdot 10^{-4}$ Pa. The maximum CO pressure for oscillations always was of the order of one tenth of the oxygen pressure so that the CO adsorption rate was lower than the O_2 adsorption rate (note the sticking coefficients in Table I). For the simulations described here, the oscillations disappear at CO pressures above $3.5 \cdot 10^{-3}$ Pa.

These results agree very well with the experimentally found data on the oxidation of CO on Pt(100); at a CO pressure of $1.6 \cdot 10^{-3}$ Pa and an oxygen pressure of $2.7 \cdot 10^{-2}$ Pa, an oscillatory region between 460 and 540 K is found,[63] with periods of oscillation between 150 and 250 seconds. Also in the experiments the oscillations disappear when the CO pressure is larger than about one tenth of the oxygen pressure; in

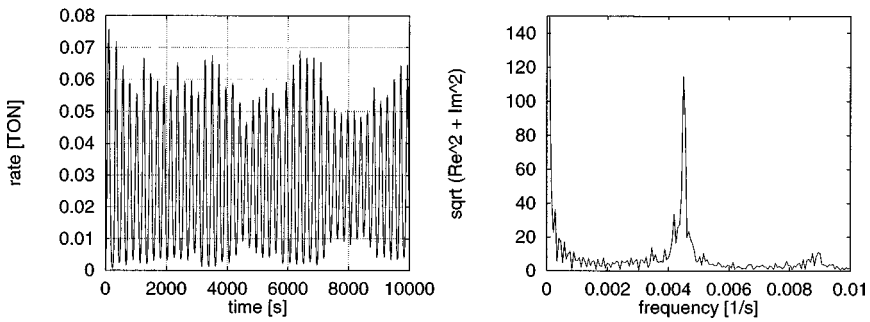

FIG. 4. Example of simulated oscillations in the production rate of CO_2 (left) and its power spectrum averaged over 10 simulation runs. Simulations at T = 490 K, grid size = 1024×1024 unit cells. Turn over numbers (TON) are in reactions per Pt atom per second. $p_{O_2} = 15.6 \cdot 10^{-2}$ Pa, $\nu(1 \times 1 \rightarrow \text{hex}) = 1.6 \cdot 10^{9}\ s^{-1}$, $E_{act}(1 \times 1 \rightarrow \text{hex}) = 105$ kJ/mol. The other rate parameters are as in Table I. No diffusion was included.

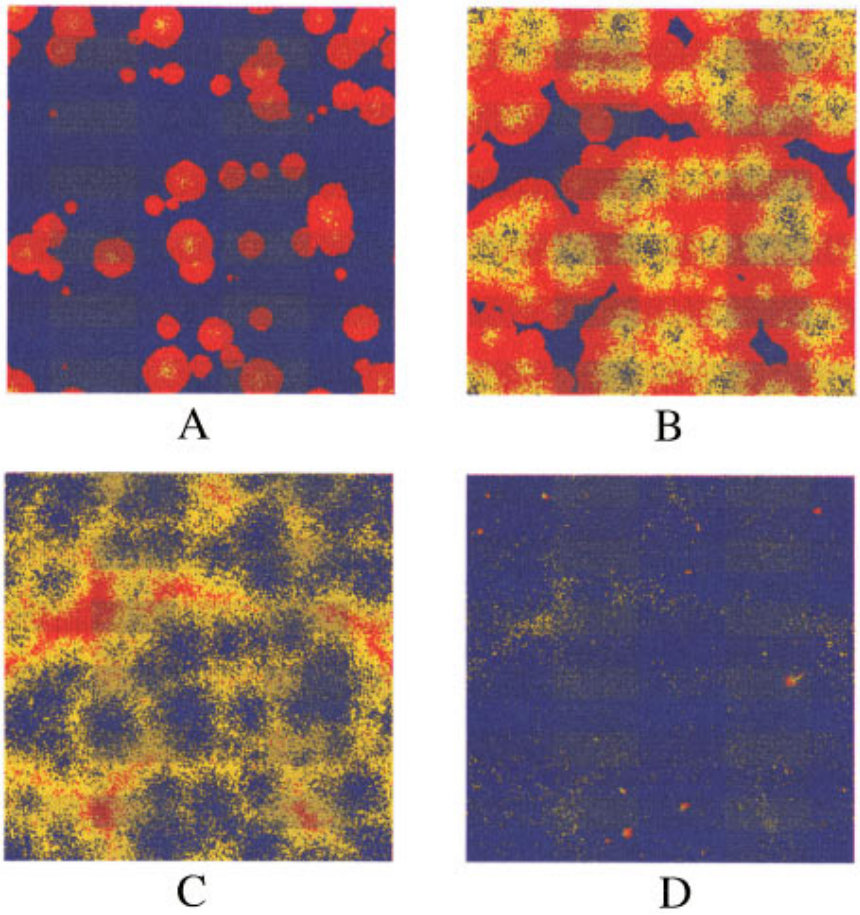

FIG. 5. (Color). Series of snapshots of a simulation grid of 1024×1024 unit cells, illustrating the observed synchronization mechanism. A number of reaction fronts arise due to CO desorption (A). When they have grown to full width, they collide (B), and extinguish one another (C). After this, an almost homogeneously transformed hexagonal phase results. On this surface, CO concentration builds up again, after which transformation into the 1×1 phase occurs (D). Red areas indicate oxygen on a 1×1 phase, blue areas indicate CO on a 1×1 phase. Yellow areas are empty hexagonal unit cells and green (mixed yellow and blue) areas show where CO is adsorbed on the hexagonal phase. Cellular structures very similar to picture (C) have been observed experimentally on Pt(110) surfaces (Ref. 19).

the experiments just mentioned, the oscillations disappeared at CO pressures above $3.6 \cdot 10^{-3}$ Pa.

The surface changes in the following way during the oscillations. When a simulation is started on an empty grid in the hexagonal phase, the only possible reaction is CO adsorption. At a certain coverage, nuclei will be formed and then the surface starts to convert into the 1×1 phase, a process we shall call the *transformation stage*. Oxygen cannot adsorb on this phase yet, because empty sites on the 1×1 phase have to be created by CO desorption. However, once two neighboring CO molecules desorb, oxygen can adsorb on this spot and when this happens, it will react with neighboring CO. The sites vacated in this reaction will be preferentially occupied by oxygen (the O_2 adsorption rate exceeds that of CO), which will again react with neighboring CO. This way, a reaction front starts to propagate over the surface. A picture of such a front can be seen in Fig. 5. We will call this the *reactive stage*. Behind the front, there is not much CO present, and oxygen adsorption will compete with 1×1 → hex transformation. Because O_2 adsorption is not possible on the hexagonal phase, the surface will now slowly transform back into the hexagonal phase, a process we will indicate with the *recovery stage*. On the hexagonal phase, only CO can adsorb and we are at the beginning of a new cycle, which starts with the transformation stage.

The completion of a cycle strongly depends on the rates chosen for the different reactions and reaction conditions. For example, when the temperature is too high, the system will be kept in the recovery stage: CO adsorption and desorption are in equilibrium, with a CO coverage that is too low to convert the whole surface into the 1×1 phase. Oxygen does adsorb frequently and then reacts with CO, but the reactive stage is not entered, because 1×1 → hex transformation is too fast, suppressing the auto-catalytic cycle of O_2 adsorption on vacant sites and subsequent creation of vacancies by reaction with CO. A temperature above 540 K will keep the CO coverage so low that the system will not even enter the transformation stage. Choosing the temperature too low causes the system to stay in the reactive stage; patches of O and CO coexist on the lattice, separated by hexagonal phase. When CO molecules adsorb on these channels, they can form a bridge between the patches, thus bringing the reactants together. On these coagulated islands, reaction is fast, and at higher temperatures, oxygen would sweep over the island, followed by transformation into the hexagonal phase. However, at lower temperatures, the 1×1 → hex re-

action is too slow to complete the transformation completely for the whole island, and as a result, oxygen patches (on 1×1 phase) remain. On the hexagonal parts, CO can adsorb again, after which again CO patches on 1×1 phase can be created. Altogether, CO_2 production is high and at steady state because of reaction between islands of reactants, but the size distribution of the patches is not changed. At very low temperatures ($T<400$ K), the surface gets poisoned by either CO or oxygen, dependent of the partial pressures and the sticking coefficients used in this temperature regime. The oscillatory region is shown in Fig. 3, where the rate of CO_2 production is plotted versus temperature. Note the peak at 490 K; at this temperature the oscillations are triggered, resulting in a high production rate in the reactive stage. The dependence of the amplitude on temperature, shown in Fig. 3 is in excellent agreement with early experiments on CO oxidation on Pt(100) reported by Ertl *et al.*[16]

The dependence of the oscillations on the rate constants of the system parameters will be discussed in the following paragraphs. The other rate parameters had little influence on the oscillatory behavior of the system.[61]

CO desorption is one of the ''triggers'' for reaction fronts; on a 1×1 surface with a very high CO coverage, oxygen cannot adsorb. When two neighboring sites are depleted by CO desorption, this empty spot can initiate a reaction front. On small grids, this triggering mechanism is essential for obtaining oscillatory behavior. On large grids (512×512 unit cells and larger), this triggering occurs at different positions at close intervals, resulting in a complete loss of global oscillations because of destructive interference of the many reaction fronts (local oscillators), unless a synchronization mechanism, e.g. provided by adsorbate diffusion, is operational. Choosing different CO desorption rates does not influence the oscillation period.

The model is very sensitive toward the $1\times1\rightarrow$ hex transformation rate. Increasing the rate of this reaction by a factor of 2 narrows the temperature window in which oscillations occur to: $470<T<490$ K. Increasing it by a factor of four narrows the window down to a small interval around 470 K. Decreasing the transformation rate narrows the temperature window too and shifts it upward. A decrease by factor of 2 shifts the window to 490 K $<T<530$ K, a decrease by a factor of ten leaves some oscillations around 530 K only.

Finally, we studied the influence of the nucleation and trapping rate on the oscillations, keeping equal rates for both reaction types. Decreasing or increasing the rates by more than a factor of 5 stops the oscillations, but for different reasons. At a lower rate, reaction fronts start traveling over the grid before it is completely in the 1×1 phase. Hexagonal islands still exist, obstructing the reaction front. The reaction front, hindered in its motion, will not travel fast enough so that new fronts appear before the whole grid has reacted, thus destroying synchronization. At higher nucleation and trapping rates, the hex $\rightarrow$ 1×1 phase is so rapid, and the recovery time of the system is so low, that new fronts can appear closely behind a previous front, which also ends oscillations. The nucleation and trapping rates influence the oscillation periods. Slower rates give longer periods and higher rates shorter periods.

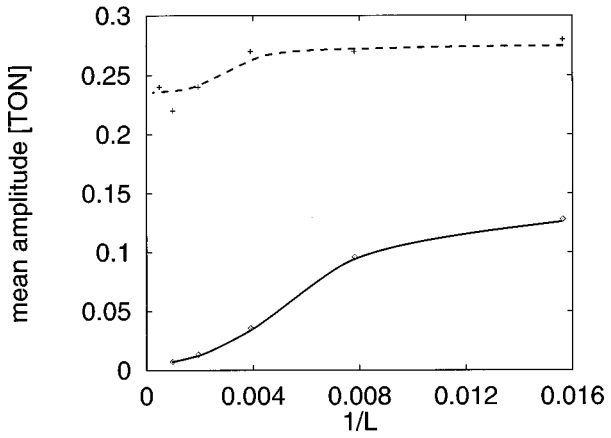

FIG. 6. Grid size dependence of average amplitudes of oscillations at 490 K. L is the linear dimension of the grid, ranging from 64 to 2048 in this plot. The solid line shows the dependence for the model without diffusion, the dashed line for the model including diffusion, with a diffusion rate constant of 30 (see Table II). Lines are only guides to the eye. On small grids, only one front is present, and oscillations seem synchronized. On large grids multiple fronts appear and local oscillations, which are out of phase, decrease the mean amplitude of the oscillations, until it vanishes for $L>1024$ if no diffusion in included. When diffusion is included, the amplitude is constant for large grids. The somewhat higher amplitude on small grids is caused by a finite size effect; a single reaction front does not fit completely on the grid. Because of that, the most reactive part of the wave covers a large part of the grid which causes higher amplitudes.

A delicate balance between the reaction rate constants determines the behavior of the system. This is illustrated by the fact that in a narrow temperature regime around 490 K, oscillations are triggered. Also the sensitivity of the oscillations to some rate parameters demonstrates this. The number of parameters is large and change of one parameter alters the behavior of the system in a non-straightforward manner.

The cause of the oscillations in our simulations is the surface transformation. Without this transformation, we would have the Ziff–Gulari–Barshad model[20] with finite reaction rates. It is well known that this model does not exhibit oscillatory behavior.[33] Surface reconstruction is not the only mechanism via which oscillations can be introduced. Site blocking by an inert species in various forms (oxide formation, carbon segregation) is known to introduce oscillations as well.[29,33] However, none of these other models have shown the quantitative agreement in temperature and pressure range and periods of oscillation with experimental observations as found with our model. Hence, it appears that the structural transformation is the dominant mechanism behind the oscillations in CO oxidation on Pt(100) surfaces.

B. Grid size effects and temporal self-organization

The grid size dependence of the average amplitudes of the oscillations is shown in Fig. 6. One observes that the oscillation amplitudes of the oscillations (dashed curve) decrease to zero with increasing grid size, which is to be expected for the following reason: the resulting average amplitude of N independent oscillators, each with a random phase shift, but equal periods, is proportional to $1/\sqrt{N}$ due to destructive interference. On the large grids we expect multiple reaction fronts present on the grid. Because the number of

fronts is proportional to the number of sites, L^2, the average amplitude will depend linearly on $1/L$. The task of a synchronization mechanism, e.g. diffusion, should be to omit the random phase shift. On small grids, we expect only one front at a time to travel across the surface and the amplitude of the oscillations will not depend on grid size.

On first sight, lowering of the CO desorption rate would imply a lower rate for the creation of two empty sites on which a new front can be initiated, and hence a higher probability for the presence of a single front on larger grids. A single front always produces synchronized, though perhaps irregular, oscillations. However, a ''self-triggering'' mechanism is dominant when CO desorption is slow (or even absent). Then after a reaction front has passed over some part of the lattice, the recovery stage starts. During this stage, some oxygen ''contaminants'' remain. These very small oxygen islands (a few atoms) are isolated by the surrounding hexagonal phase, which enters the transformation stage (CO coverage has built up, and the surface is transforming into the 1×1 phase). When the CO coverage is high enough, the oxygen can trigger a new reaction wave. Multiple reaction fronts are always present on large grids. These reaction fronts are of nanometer to micrometer scale, which is the largest scale we can simulate at present with our method.

Although our results show regular oscillations even on the largest grids we have simulated on (4096×4096 unit cells), the plots of amplitude vs $1/L$ show that in the absence of diffusion, a synchronization mechanism is missing.

The global—global means in this case for the whole grid—oscillations on our simulations grids are produced when we create circumstances such that the distance between the initiated fronts is not larger than the width of the fronts. The leading edges of the fronts then meet at a moment when CO coverage is still low. Almost the whole grid is now in the reactive stage, and the reactions that occur are mainly adsorption of CO and O_2, production of CO_2 and $1\times1 \rightarrow$hex transformation. Because of the transformation reactions, the reaction stops: oxygen does not adsorb on the hexagonal grid, and depletion of one of the reactants will extinguish the reaction. Subsequently, CO coverage can build up, whereafter the surface can transform into the square phase, on which new reaction fronts can be initiated by CO desorption. This brings us back to the beginning of the cycle. This way, oscillations are synchronized on a local scale, up to grids of 1024×1024 unit cells. One should note that this is not a synchronization mechanism that forces many local oscillators to oscillate in phase, but rather a mechanism that periodically annihilates all local oscillations. It is unstable to local disturbances. A more detailed description of this mechanism is given in Sec. IV C.

When stochastic fluctuations cause part of the grid to produce a few reaction fronts earlier than on the rest of the grid, this part of the grid will enter the recovery stage earlier. As a result, a patch will appear which looks ''wiped clean''; because this part is in the recovery stage, no reaction fronts are present, whereas the rest of the grid is covered with these fronts. These other fronts cannot penetrate the ''clean'' patch because of the high concentration of hexagonal sites. As a result, the clean patch will grow and pattern formation will occur, either in the form of turbulent wave patterns or in the form of rotating spirals and target patterns. On large grids, the probability for local disturbances to occur will increase and hence the oscillation amplitudes will vanish on infinite grids. This implies that we observe finite size effects even on our largest grids.

C. Spatio-temporal pattern formation

Several forms of spatio-temporal pattern formation were observed in our simulations. We discern two types of patterns: patterns of type I are observed *during* oscillations and patterns of type II are observed under *steady state* conditions. Type I patterns observed in experiments include cellular patterns and standing waves, type II patterns include target patterns, spirals and turbulent patterns.[18,25] Note that both types of pattern formation may occur under exactly the same macroscopic circumstances (temperature, partial pressures).

The type I pattern formation we have observed are cellular patterns, as depicted in Fig. 5. These patterns are a manifestation of the front collisions. At many spots on the grid, reaction waves are initiated. These fronts grow and at a certain moment they collide. When small fronts collide at the moment only part of the surface is covered with fronts, these fronts can melt together and form a single, larger front. When most of the surface is covered with fronts, they cannot melt together and colliding fronts will extinguish. At that moment the cells are at maximum size. Cell walls are formed by oxygen adsorbates and hexagonal (unreactive) phase. These patterns are qualitatively very similar to experimentally observed patterns on Pt(110) surfaces.[19] As in the experiments, the cells are only observed simultaneously with global oscillations in CO_2 production.

Without diffusion, the cellular structure is not stable. It can only be observed on grids large enough to contain multiple cells. The local synchronization mechanism which produces the structure breaks down easily on these large grids because local fluctuations grow out and form patterns of type II. These patterns include target patterns, (double) rotating spirals and turbulent patterns, as shown in Fig. 7. Target patterns and rotating spirals are quite stable. However, when they grow large enough to cover the whole grid, they interfere with themselves through the periodic boundary conditions, which causes them to break down into turbulent patterns, which are very stable. The stability of target patterns and spirals is increased by omission of the periodic boundaries. All of the patterns we have observed have also been reported from experiments for CO oxidation on Pt(110) surfaces, be it at larger scale.[18,19,64–67] Similar patterns on the Pt(100) surface have not been observed in CO oxidation, although the CO + NO reaction does show pattern formation on this surface.[68] MC simulations by Goodman *et al.*[40] also have shown appearance of spirals and target patterns.

In target patterns, new reaction fronts emanate regularly from a seemingly fixed spot on the surface. Our simulations show that this is only apparently the case. In fact, new fronts are not initiated regularly in time and not at the same place at all. Concentration gradients of adsorbates and surface phases stabilize the pattern and cause the apparent periodicity both in time and place. The mechanism is as follows. First, the

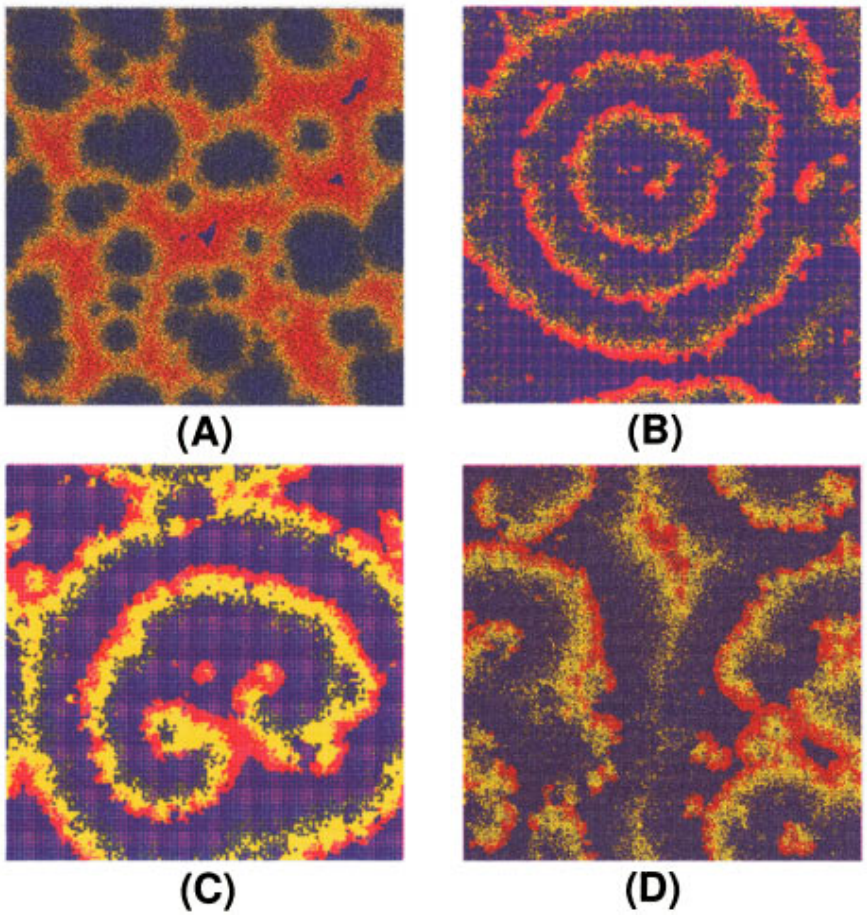

FIG. 7. (Color). Pattern formations during our simulations on grids of 1024 × 1024 unit cells. (A) Cellular patterns, (B) target patterns, (C) a double spiral, (D) turbulent patterns. The cellular patterns in this figure were obtained with diffusion. Colors as in Fig. 5.

target pattern is created by the mechanism described in Sec. IV B. Suppose we start with one ring-shaped reaction front as sketched in Fig. 8 together with its concentration profiles. We call this front the *primary front* and it was initiated at the *primary spot*. At random positions on the surface new fronts will be initiated after desorption of two neighboring CO molecules. Fronts that are initiated outside the primary front will be overtaken and they will melt together with the much larger primary front. Now we consider a newly initiated front close to the primary front, but inside it. This front can either

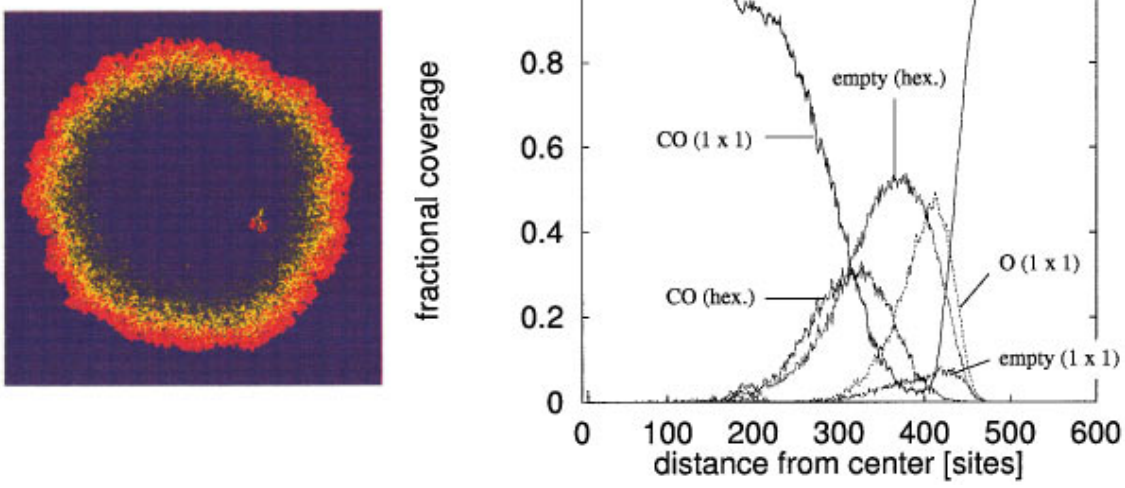

FIG. 8. (Color). Concentration profiles of adsorbate coverages and surface phases for a single reaction front. Note the initiation of a new reaction front inside the ring. This front is not initiated in the center of the primary front, but will be reshaped into a concentrical circle. Colors as in Fig. 5.

be generated by desorption of CO or by the self-triggering mechanism (Sec. VI). This front will grow in all directions, however, in the direction of the primary front it will be slowed down because it is hindered by the increasing concentration of hexagonal phase (when this concentration is too high the front will die). In the opposite direction it is accelerated because of a decreasing concentration of hexagonal phase. Its propagation rate in this direction will be high until it encounters a high concentration of hexagonal phase, which is at a certain fixed distance from the primary front. When meanwhile a new front is initiated inside the primary front, the small fronts will melt together. Thus, each front that is initiated inside the primary front is reshaped into a circle around the primary center, and after some time it will travel at a fixed distance from the primary front. Hence we have a self-organizing process, keeping the pacemaker in place. The front distance, as well as the front width, is determined by the values of the rate constants. At the rate parameters of Table I, the distance is around 200 unit cells, which would correspond to ca. 0.05 μm on Pt(100). This is ten to hundred times smaller than the experimental values[18,19,64–67] obtained on Pt(110).

Target patterns are stabilized by surface inhomogeneities with a high higher oxygen affinity. Surface defects have been proposed to fulfill such a role.[18] If we introduce a spot on the grid which has a higher affinity for oxygen than the rest of the grid, this spot acts as a fixed front initiator. From this spot, reaction fronts are emanated and front reshaping by concentration gradients again causes apparent periodicity. The spatio-temporal pattern formation created this way, is more stable than in the absence of defects. Furthermore, the patterns extend more quickly over a large area. This agrees with the observation[18] that structural defects on the surface can introduce spatio-temporal pattern formation. However, our simulations show that structural defects form a stabilizing, rather than a necessary factor.

Rotating spirals are stabilized by a similar mechanism, and their creation also occurs spontaneously. A small reaction front spontaneously starts rotating around a ''core,'' which sometimes meanders across the surface. When spirals are small, their rotating ''head'' collides with the ''tail'' which separates the two. The head keeps rotating while tail is reshaped into a circular front. As the spiral grows, both the head and the tail become larger and the spiral can grow out to the size of the grid. Sometimes, the tail starts to curl back before that time, and a double spiral results. Double spirals have also been reported in the literature, e.g. in Ref. 66. Again, the length scale of the patterns in our simulations is 10–100 times smaller than in experiments.

All type II pattern formations destroy oscillations, resulting in steady state CO_2 production, as also found in experiments by several groups.[18,19] One should note that our pattern formation is not a consequence of interference across the boundary conditions, as proved by the fact that they are more stable on larger grids. Furthermore, in one simulation, we have used a grid without periodic boundary conditions, which made spirals more stable and makes it easier for them to grow (have more windings).

TABLE II. Values for the rate parameters used in simulations which include diffusion. Symbols as in Table I. The rate constants for diffusion were chosen temperature independent. At 490 K, at which almost all simulations were done, the effective normalized rates are, when a diffusion rate of 30 is chosen, for CO adsorption: $3.1\cdot10^{-5}$; for oxygen adsorption: $7.6\cdot10^{-5}$; for CO desorption: $2.1\cdot10^{-4}$; for CO_2 production: $4.2\cdot10^{-1}$; for $1\times1\rightarrow$ hexagonal reconstruction: $2.9\cdot10^{-4}$; for nucleation and trapping: $2.9\cdot10^{-4}$ and for diffusion: $5.7\cdot10^{-1}$.

Reaction	p^{sim} (Pa)	S_0^{sim}
CO ads.	$2.0\cdot10^{-3}$	0.8
O_2 ads.	$4\cdot10^{-2}$	0.1
	ν^{sim} (s^{-1})	E_{act}^{sim} (kJ/mol)
CO des.	$1\cdot10^{15}$	159
CO_2 prod.	$2\cdot10^{10}$	84
$1\times1\rightarrow$ hex	$1.6\cdot10^{9}$	97
Nucleation	0.015	0
Trapping	0.015	0
Diffusion rate constants	10-50	0

D. Influence of diffusion

Diffusion has been included in our model as an elementary reaction which swaps the labels of two neighboring sites. One of the sites must be empty (S or H label) and the other site must have a CO label. We have only simulated diffusion with the model in which CO adsorbs on top sites. Thus, an example of a reaction would be (CO, S) + (S, S) $\rightarrow$ (S, S) + (CO, S), or (CO, S) + (H, H) $\rightarrow$ (S, S) + (CO, H). We have chosen the diffusion rate temperature independent. Diffusion rates are considered to be the same for the hexagonal and the 1×1 phase and diffusion is not hindered by phase boundaries. Inclusion of diffusion in our model still produces oscillations and spatio-temporal pattern formations in the same temperature regime. In fact, diffusion introduces few qualitative changes in the behavior of our system. The changes are briefly discussed below.

First of all, inclusion of diffusion alters the rate parameters for some elementary reactions at which oscillations are found. The rate parameters used with diffusion are given in Table II. Especially the CO desorption rate constant has to be increased to a value which is more in agreement with experimental values. The self-triggering mechanism becomes suppressed because small oxygen islands now are no longer isolated by hexagonal phase. CO desorption is now the only trigger for front initiation. Pairs of empty sites created by desorption now are often separated by diffusion before front initiation can occur. We therefore expect CO desorption and diffusion to influence the period of the oscillations. Indeed this is found; faster CO desorption (enhanced empty pair creation) causes shorter periods, and faster diffusion (diminished empty pair creation) causes longer periods. In the limit of very high diffusion rates (when the mean free path for adsorbates is larger than the grid) one would expect the number of empty pairs to become independent of diffusion rate, since diffusion annihilates as well as generates empty site pairs.

A second reason for the longer period with high diffu-

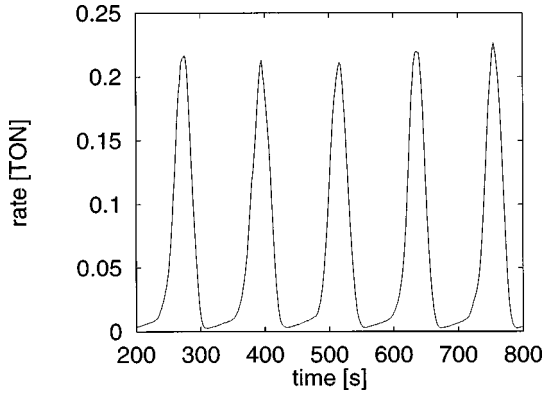

FIG. 9. Oscillations in CO_2 production rate with diffusion (rate: 30 s^{-1}) included in the model.

sion rates is that the hex $\rightarrow 1\times1$ reconstruction is delayed, because CO-clusters dissolve more rapidly. Together with the empty pair separation, this causes the recovery stage, in which the amount of CO and 1×1 phase builds up on the surface, to become longer. This is clearly visible in Fig. 9 from the tails in the CO_2 production peaks. Without diffusion, these tails are absent. Initial results indicate that the homogeneous CO coverage prevents formation of 1×1 nuclei until the CO coverage is very high, and reconstruction then proceeds very fast.

Diffusion synchronizes oscillations on large grids. This could be due to the fact that the length scale of the (cellular) pattern formation has increased, implying that the breakdown of synchronization has shifted to grid sizes which are too large for our simulations. Our first results suggest another, unexpected way of synchronization, which will be explained below.

First of all, during oscillations, the cellular patterns are still present and they are even more pronounced than without diffusion. CO molecules inside the cells can diffuse around, which makes the CO coverage inside the cells more homogeneous. CO cannot penetrate the cell walls, because these are too reactive. After the cell walls have ''dissolved,'' when the oxygen cell walls have reacted away, CO molecules can suddenly diffuse into neighboring cells. At this stage, cell walls are still present as hexagonal phase, but this forms no barrier for diffusion. From this moment, the recovery stage begins in which diffusion makes the CO coverage homogeneous across the whole surface, thus erasing the hexagonal phase remaining from the cells. At the same time, CO coverage increases. The surface is still mostly in the hexagonal phase, because diffusion delays the hex $\rightarrow 1\times1$ reconstruction. This stage becomes longer with increasing diffusion rate. Because this stage is so long, the CO coverage can become homogeneous after each oscillation cycle. New fronts are generated at random positions and the longer the recovery stage takes, the more fronts are generated because of the increased CO coverage (meaning that more CO desorption takes place). As long as reconstruction has not set in yet, all fronts will die from too high concentrations of hexagonal phase. When reconstruction has set in though, growing fronts start at random positions and at random moments in time. These fronts collide and extinguish after which the surface is homogenized. Hence, in this mechanism, synchronization is not achieved by increasing the length scale of the processes on the surface, but by homogenization of the coverages *after* the reactive stage has ended. During the reactive stage, the effect of diffusion is limited to an increase of the length scale of the patterns. Qualitative differences only appear after the cell walls have dissolved.

Initial simulations with different diffusion rates suggest that a power-law dependence holds for the cell sizes and the oscillation period. Further investigations are essential to determine whether these grow with the same exponent or not and whether this dependence holds in a wide range of diffusion rates. We could then study whether our results can be extrapolated to realistic diffusion rates—which are 10^5–10^6 times higher—and study the implications for the sizes of the patterns.

We have observed some type II patterns with the model including diffusion. Starting target pattern formation occurred on a 1024×1024 grid with diffusion, but these patterns were not stable because of interference across the boundaries. Also these patterns seem to grow with higher diffusion rates. We will need to simulate on larger grids (at least 2048×2048 sites) to prevent interference across the grid boundaries to study the influence of diffusion on this pattern formation properly.

Finally, we found that with diffusion, the system has become much less sensitive to the values of most rate parameters, which may be due to the increased synchronization of the oscillations.

V. DISCUSSION AND CONCLUSIONS

Without diffusion, our system represents an excitable medium with spatio-temporal pattern formation and unstable oscillations.[69] The stage in which reaction fronts propagate over the surface, a stage we described as the *reactive stage* in Sec. IV A, corresponds to the excited state of the medium. Although no explicit diffusion is included, spatio-temporal pattern formation is observed. In contrast, reaction-diffusion models based on ODEs have clearly shown that diffusion terms are necessary to describe pattern formation. The explanation of this paradox has been given by e.g. Goodman *et al.*[40] They have shown that the propagation of our simulated fronts can in principle be described by an effective diffusion constant:

$$v = a\sqrt{k_{\mathrm{eff}} D_{\mathrm{eff}}}, \tag{5}$$

where v is the front velocity, k_{eff} an effective reaction rate constant and D_{eff} an effective diffusion constant. In the absence of explicit diffusion, D_{eff} is in our case due to the reaction-driven front propagation. D_{eff} and k_{eff} can be extracted from simulations with a fitting procedure. Goodman *et al.*[40] used this approach to study the dependence of wave velocity on diffusion for an adapted Ziff, Gulari and Barshad (ZGB) model.[20]

Without diffusion, the main predictions of our model are pattern formation and oscillations which are synchronized on small grids only. Though these results are interesting from a model point of view and for small particles or surfaces as in

FEM experiments,[70] comparison with experiments is hampered because diffusion is absent and the rate for CO desorption in our simulations is much too slow.

The grid size dependence we find shows that for Monte Carlo studies on kinetic oscillations one should be very careful in concluding that one has found oscillations. Checking grid size effects by increasing the grid dimensions by a factor of two or four is often used, but this is clearly not enough. Grid size effects should therefore be checked more thoroughly and on much larger grids. Furthermore, our results suggest that irregular oscillations simulated on small grids[21,24,39,40] will vanish on large grids. The concomitant pattern formations may have to be attributed to finite grid size effects.

To check this hypothesis, we have reproduced the results of Ertl's group[21,39] with our model. On the same grids (17×40 and 20×78 grids with no periodic boundary conditions) we also found irregular oscillations and wave trains. However, these phenomena disappeared completely on large periodic grids (1024×1024). Hence we can attribute them to fluctuations rather than sustained oscillations.

The cellular structures we found in our simulations are of the same form as those found on Pt(110) surfaces by Rose *et al.*[19] They are not to be confused with standing waves or Turing structures. In each oscillation cycle, our cells appear at random positions and after each cycle the patterns are erased. This erasure is incomplete when diffusion is absent, which causes the system to ''remember'' the positions of the cells and new cells have a preference to re-appear at the same position. This memory effect is caused by oxygen remnants which are isolated by hexagonal phase. Diffusing CO molecules find no barrier in this hexagonal phase and will react with the oxygen remnants after diffusion towards them. This completely erases the system's memory and thus synchronizes oscillations.

The most striking fact of the type II pattern formations is that the pattern formation (both concentrical wave fronts and rotating spirals) emerge from several fronts which spontaneously cooperate, despite their random positions and phase with respect to one another. After creation of the pacemaker, it is stabilized by a self-stabilizing mechanism. Furthermore, during a simulation, target patterns can change into rotating spirals and vice versa.[71] We conclude that no inhomogeneities, lateral interactions or communication mechanisms on a large length scale are required for any of these effects, although structural defects on the surface stabilize and pin down the patterns. Diffusion or any other synchronization mechanism is not required for the pattern formations to occur. The pattern formation is not an artifact of our simulation technique nor of our model without diffusion. The smaller scale is due to the absence of fast diffusion, but consistent with the excitable nature of our system.

Although realistic diffusion rates cannot be simulated with the method we are using, valuable information on the role of diffusion can be obtained. The quantitative results become more in agreement with experiments; the rate constants in the oscillatory regime have more realistic values in the presence of diffusion and the length scales of the pattern formations increases.

In summary, we have developed a model which includes detailed elementary reaction steps for the oxidation of CO on single crystal surfaces. Even when no diffusion is incorporated, this model reveals many features generally observed in catalytic reactions on single crystal surfaces. These features include regular oscillations on a small length scale (up to 1 μm) and several types of spatio-temporal pattern formation. The time scales are in agreement with experimental observations. Incorporation of diffusion introduces a synchronization mechanism and increases the length scales of all phenomena increase and more realistic rate parameters can be used.

ACKNOWLEDGMENT

We gratefully acknowledge Tom Verhoeff of the Department of Mathematics and Computing Science of Eindhoven University of Technology for providing invaluable computer resources.

[1] R. A. van Santen and M. Neurock, Catal. Rev. Sci. Eng. **37**, 557 (1995).
[2] B. Hammer and J. Nørskov, Surf. Sci. **343**, 211 (1995).
[3] B. Hammer and J. Nørskov, Nature (London) **376**, 238 (1995).
[4] H. Burghgraef, A. P. J. Jansen, and R. A. van Santen, Surf. Sci. **324**, 345 (1995).
[5] Y. S. Li, M. A. van Daelen, J. M. Newsam, and R. A. van Santen, J. Phys. Chem. **100**, 2279 (1996).
[6] D. T. Gillespie, J. Comput. Phys. **22**, 403 (1976).
[7] D. T. Gillespie, J. Phys. Chem. **81**, 2340 (1977).
[8] A. P. J. Jansen, Comput. Phys. Commun. **86**, 1 (1995).
[9] K. A. Fichthorn and W. H. Weinberg, J. Chem. Phys. **95**, 1090 (1991).
[10] B. Meng and W. H. Weinberg, J. Chem. Phys. **100**, 5280 (1994).
[11] H. C. Kang and W. H. Weinberg, Acc. Chem. Res. **25**, 253 (1992).
[12] J. Lukkien, J. P. L. Segers, P. A. J. Hilbers, R. J. Gelten, A. P. J. Jansen, and R. A. van Santen (unpublished).
[13] G. Ertl, Adv. Catal. **37**, 213 (1990).
[14] R. Imbihl, Prog. Surf. Sci. **44**, 185 (1993).
[15] R. Imbihl and G. Ertl, Chem. Rev. **95**, 697 (1995).
[16] G. Ertl, P. R. Norton, and J. Rüstig, Phys. Rev. Lett. **49**, 177 (1982).
[17] R. Imbihl, M. P. Cox, G. Ertl, H. Müller, and W. Brenig, J. Chem. Phys. **83**, 1578 (1985).
[18] S. Jakubith, H. H. Rotermund, W. Engel, A. von Oertzen, and G. Ertl, Phys. Rev. Lett. **65**, 3013 (1990).
[19] K. C. Rose, D. Battogtokh, A. Mikhailov, R. Imbihl, W. Engel, and A. M. Bradshaw, Phys. Rev. Lett. **76**, 3582 (1996).
[20] R. M. Ziff, E. Gulari, and Y. Barshad, Phys. Rev. Lett. **24**, 2553 (1986).
[21] P. Möller, K. Wertzl, M. Eiswirth, and G. Ertl, J. Chem. Phys. **85**, 5328 (1986).
[22] K. Fichthorn, E. Gulari, and R. Ziff, Chem. Eng. Sci. **44**, 1403 (1989).
[23] D. G. Vlachos, F. Schüth, R. Aris, and L. D. Schmidt, Physica A **188**, 302 (1992).
[24] X.-G. Wu and R. Kapral, Physica A **188**, 284 (1992).
[25] H. Rosé, H. Hempel, and L. Schimansky-Geier, Physica A **206**, 421 (1994).
[26] A. L. Vishnevskii, E. I. Latkin, and V. I. Elokhin, Surf. Rev. Lett. **2**, 459 (1995).
[27] J. P. Boon, D. Dab, R. Kapral, and A. Lawniczak, Phys. Rep. **273**, 55 (1996).
[28] R. Kapral and X. G. Wu, J. Phys. Chem. **100**, 18976 (1996).
[29] A. P. J. Jansen and R. M. Nieminen, J. Chem. Phys. **106**, 2038 (1997).
[30] J. P. Hovi, A. P. J. Jansen, and R. M. Nieminen, Phys. Rev. E **55**, 4170 (1997).
[31] R. Danielak, A. Perera, M. Moreauy, M. Frankowicz, and R. Kapral Physical A (submitted).
[32] A. P. J. Jansen, J. Mol. Cat. A: Chemical **119**, 125 (1997).
[33] M. M. Slin'ko and N. I. Jaeger, *Oscillating Heterogeneous Catalytic Systems* (Elsevier, Amsterdam, 1994).
[34] N. A. Collins, S. Sundaresan, and Y. Chabal, Surf. Sci. **180**, 136 (1987).
[35] V. A. Burrows, S. Sundaresan, Y. J. Chabal, and S. B. Christman, Surf. Sci. **180**, 110 (1987).
[36] C. G. Vayenas and J. N. Michaels, Surf. Sci. **120**, L405 (1982).

[37] M. R. Basset and R. Imbihl, Chem. Phys. **93**, 811 (1990).
[38] A. L. Vishnevskii, V. I. Elokhin, and M. L. Kutsovskaya, React. Kinet. Catal. Lett. **51**, 211 (1993).
[39] M. Eiswirth, P. Möller, K. Wetzl, R. Imbihl, and G. Ertl, J. Chem. Phys. **90**, 510 (1989).
[40] R. H. Goodman, D. S. Graff, L. M. Sander, P. Leroux-Hugon, and E. Clément, Phys. Rev. E **52**, 5904 (1995).
[41] M. P. Cox, G. Ertl, and R. Imbihl, Phys. Rev. Lett. **54**, 1725 (1985).
[42] K. Krischer, M. Eiswirth, and G. Ertl, J. Chem. Phys. **96**, 9161 (1992).
[43] A. Hopkinson and D. A. King, Chem. Phys. **177**, 433 (1993).
[44] M. Gruyters, T. Ali, and D. King, Chem. Phys. Lett. **232**, 1 (1995).
[45] M. Markus and B. Hess, Nature (London) **347**, 56 (1990).
[46] M. Gerhardt, H. Schuster, and J. J. Tyson, Science **247**, 1563 (1990).
[47] PIZZAZZ is a general-purpose program, written in C++, for simulating reactions on surfaces that can be represented by regular grids. It is an implementation of the first-reaction method, written by A.P.J. Jansen.
[48] CARLOS is a general-purpose program, written in C, for simulating reactions on surfaces that can be represented by regular grids. It is an implementation of both the first-reaction method and the variable stepsize method, written by J.J. Lukkien.
[49] J. L. Sales, R. O. Uñac, M. V. Gargiulo, V. Bustos, and G. Grablich, Langmuir **12**, 95 (1996).
[50] A. E. Reynolds, D. Kaletta, G. Ertl, and R. J. Behm, Surf. Sci. **218**, 452 (1989).
[51] M. Tammaro, M. Sabella, and J. W. Evans, J. Chem. Phys. **103**, 10277 (1995).
[52] P. A. Thiel, R. J. Behm, P. R. Norton, and G. Ertl, J. Chem. Phys. **78**, 7448 (1983).
[53] T. E. Jackman, K. Griffiths, J. A. Davies, and P. R. Norton, J. Chem. Phys. **79**, 3529 (1983).
[54] P. A. Thiel, R. J. Behm, P. R. Norton, and G. Ertl, Surf. Sci. **121**, L553 (1982).
[55] R. J. Behm, P. A. Thiel, P. R. Norton, and G. Ertl, J. Chem. Phys. **78**, 7437 (1983).
[56] E. Ritter, R. J. Behm, G. Pötschke, and J. Wintterlin, Surf. Sci. **181**, 403 (1987).
[57] P. Gardner, R. Martin, M. Tüshaus, and A. M. Bradshaw, J. Electron Spectrosc. Relat. Phenom. **54/55**, 619 (1990).
[58] A. Borg, A. M. Hilmen, and E. Bergene, Surf. Sci. **306**, 10 (1994).
[59] D. A. King, Surf. Rev. Lett. **1**, 435 (1994).
[60] A. Hopkinson, J. M. Bradley, X. C. Guo, and D. King, Phys. Rev. Lett. **71**, 1597 (1993).
[61] R. J. Gelten, A. P. J. Jansen, R. A. van Santen, J. J. Lukkien, J. P. L. Segers, and P. A. J. Hilbers (unpublished).
[62] A. T. Pasteur, X.-C. Guo, T. Ali, M. Gruyters, and D. A. King, Surf. Sci. **366**, 564 (1996).
[63] M. Eiswirth, R. Schwankner, and G. Ertl, Z. Phys. Chem. N. F. **144**, 59 (1985).
[64] F. Mertens, R. Imbihl, and A. Mikhailov, J. Chem. Phys. **101**, 9903 (1994).
[65] K. Asakura, J. Lauterback, H. H. Rotermund, and G. Ertl, J. Chem. Phys. **102**, 8175 (1995).
[66] K. C. Rose, R. Imbihl, B. Rausenberger, C. S. Rastomjee, W. Engel, and A. M. Bradshaw, Surf. Sci. **354**, 258 (1996).
[67] H. H. Rotermund, G. Haas, R. U. Franz, R. M. Tromp, and G. Ertl, Science **270**, 608 (1995).
[68] G. Veser and R. Imbihl, J. Chem. Phys. **96**, 7155 (1992).
[69] A. S. Mikhailov, *Foundations of Synergetics I* (Springer-Verlag, Berlin, 1994).
[70] M. F. H. van Tol, P. T. Wouda, and B. E. Nieuwenhuys, J. Vac. Sci. Technol. A **12**, 2176 (1994).
[71] A movie (mpeg-format), and some snapshots from it, can be found on the World Wide Web at URL: http://www.tak.chem.tue.nl/theory/, under the research projects of the first author.
[72] M. A. Barteau, E. I. Ko, and R. J. Madix, Surf. Sci. **102**, 99 (1981).
[73] P. R. Norton, K. Griffiths, and P. E. Bindner, Surf. Sci. **138**, 125 (1984).
[74] A. Hopkinson, X. C. Guo, J. M. Bradley, and D. A. King, J. Chem. Phys. **99**, 8262 (1993).
[75] C. T. Campbell, G. Ertl, H. Kuipers, and J. Segner, J. Chem. Phys. **73**, 5862 (1980).
[76] Y. Y. Yeo, C. E. Wartnaby, and D. King, Science **268**, 1731 (1995).
[77] M. A. Barteau, E. I. Ko, and R. J. Madix, Surf. Sci. **104**, 161 (1981).
[78] P. R. Norton, J. A. Davies, D. K. Creber, C. W. Sitter, and T. E. Jackman, Surf. Sci. **108**, 205 (1981).